Wiley Online Library
Early View publication on www.wileyonlinelibrary.com
(issue and page numbers not yet assigned;
citable using Digital Object Identifier – **DOI**)

Phys. Status Solidi C, 1700127 (2017) / **DOI** 10.1002/pssc.201700127

physica status solidi c
www.pss-c.com
current topics in solid state physics

Ab initio study of electronic structure and magnetic properties of CoMnTaZ (Z = Si, Ge) quaternary Heusler compounds

Mourad Attallah[1], Miloud Ibrir[2], Saadi Berri*[,3], and Said Lakel[1]

[1] Department of Physics, Faculty of Sciences, University of Biskra, Algeria
[2] Department of Physics, Faculty of Sciences, University of Msila, Algeria
[3] Laboratory for Developing New Materials and their Characterizations, University of Setif 1, Algeria

Received 27 March 2017, accepted 30 May 2017
Published online 13 June 2017

Keywords *ab initio* calculations, FP-LAPW, half-metallic, Heusler compounds, spintronic

* Corresponding author: e-mail berrisaadi12@yahoo.fr, Phone: +213 95 11 55 76, Fax: +213 36 92 72 10

The electronic structures and magnetic properties of CoMnTaSi and CoMnTaGe Heusler alloys with LiMgPbSb-type structure investigated firstly by using the first-principles calculations. We have applied the full-potential linearized augmented plane waves plus local orbitals (FP-L/APW+LO) method. Exchange-correlation effects are treated using the generalized gradient approximations GGA and GGA+U. The GGA calculation shows the CoMnTaSi and CoMnTaGe compounds at its equilibrium lattice constant are HM ferromagnet with an indirect band gap $\Gamma \rightarrow X$ of 0.34 and 0.39 eV and a HM gap of 0.34 and 0.13 eV in the spin-down channel. The CoMnTaZ (Z = Si, Ge) compounds have an integer total magnetic moment of 1.00 μ_B, satisfying the Slater–Pauling rule $m_{tot} = (Nv - 24)$. The similar results are also obtained by GGA+U calculation. Therefore, these new materials are good candidates for potential applications in spintronic.

1 Introduction Numerous investigations have been extensively done regarding the Heusler compounds structure with different compositions and structures, motivated by their possible applications in spintronics [1–5]. They have shown a wide range of attractive properties such as magnetoresistance [6–8], non-local spin-valve devices [9, 10], spin injectors to semiconductors [11], and magnetic tunnel junctions [12, 13].

Half-metallic ferromagnets (HMFs) meet all the requirements of spintronics, as a result of their exceptional electronic band structure [14]. These materials behave like metals with respect to the electrons of one spin direction and like semiconductors (or insulator) with respect to the electrons of the other spin direction [15]. The first material which was predicted to be a half-ferromagnet was the half-Heusler alloy NiMnSb found by de Groot and co-workers [16] in 1983. Various half-metallic ferromagnetism have been predicted by the first-principles calculations or experimentally synthesized, such as double perovskites [17–26], zinc blende (ZB) II–V or II–IV compounds [27–30], Heusler alloys [31–37], and ferromagnetic manganites $La_{2/3}Sr_{1/3}MnO_3$ [38, 39]. Magnetite, Fe_3O_4, is thought to be a half-metallic ferrimagnet [32].

The Zr-based quaternary Heusler alloys, ZrCoTiZ (Z = Si, Ge, Ga, and Al), ZrFeTiZ (Z = Al, Si, and Ge), and ZrNiTiAl have been reported to be HMF very recently [40, 41]. This is the first prediction of HMF in the 4d transition metal elements for the Zr-based quaternary alloys. Many quaternary Heusler compounds are found to possess the half-metallic band structure as revealed by the ab-initio calculations [42–46]. Rasool et al. [47] calculated the structural, magnetic, and electronic properties of YCoCrZ (Z = Si, Ge, Ga, and Al) using full-potential linearized augmented plane wave (FPLAPW) scheme within the GGA. The electronic structure calculations predicted a HMF band structure for YCoCrZ (Z = Si, Ge, Ga, and Al), with half-metallic gap of 0.70, 0.65, 0.46, and 0.35 eV for YCoCrSi, Ge, Ga, and Al, respectively. The calculated total magnetic moment 4.00 and 3.00 μ_B for

YCoCrSi, Ge and YCoCrGa, Al, respectively, found to agree with Slater–Pauling rule [48–50]. Wang et al. [51] and Liu et al. [52] also predicted that ZrVTi (Al, Ga) and ZrTiCr (Al, Ga, and In) quaternary Heusler compounds were HM ferromagnets. Xie et al. [53] calculated magnetic and electronic structure of ZrMnVZ and ZrCoFeZ (Z = Si, Ge) using full full-potential local-orbital (FPLO) minimum-basis band-structure method within the GGA. The electronic structure calculations predicted a HMF band structure for ZrMnVZ and ZrCoFeZ (Z = Si, Ge), with half-metallic gap of 0.14, 0.18, and 0.22 eV for ZrMnVSi, ZrMnVGe, and ZrCoFeSi, respectively.

In recent reports [54–56], some so-called LiMgPdSn or Y-type structure Heusler alloys with a formula of XX'YZ have been discovered to be spin-gapless semiconductors (SGS) by first-principle calculations. Very recently, Wang et al. [57, 58] and with his colleague have studied ZrFeVZ (Z = Al, Ga, and In) and ZrRhHfZ (Z = Al, Ga, and In) alloys which exhibited HMF characteristic in their electronic structures basing on first-principles calculation.

The main goal of the present work is to obtain report on the structural, electronic, and magnetic properties of quaternary Heusler CoMnTaSi and CoMnTaGe in LiMgPdSn-type crystal structure with the space group F4-3m. In this structure, Co, Mn, Ta, (Si or Ge) atoms are placed on the Wyckoff positions 4a(0,0,0), 4d(1/2,1/2,1/2), 4c (1/4,1/4,1/4), and 4b(3/4,3/4,3/4), respectively. The crystal structure of these compounds is shown in Fig. 1. The calculations are performed using *ab initio* full-potential linearized augmented plane wave (FP-LAPW) within the density functional theory DFT within the generalized gradient approximation GGA and GGA+U methods. Our paper is organized as follows. The theoretical background is presented in Section 2. Results and discussion are presented in Section 3. A summary of the results is given in Section 4.

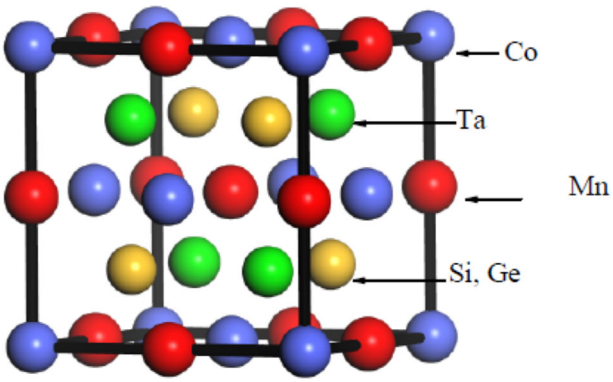

Figure 1 Crystal structure of CoMnTaZ (Z = Si, Ge) quaternary Heusler compounds.

2 Method of calculations Self-consistent FP-LAPW [59, 60] calculations on CoMnTaZ were carried out using WIEN2k package [61]. Both the generalized gradient approximation GGA [62] and GGA+U [63]. The Kohn–Sham equations are solved self-consistently using FP-LAPW method. In the calculations reported here, we use a parameter $R_{MT}K_{max} = 7$, which determines matrix size (convergence), where K_{max} is the plane wave cut-off and R_{MT} is the smallest of all atomic sphere radii for CoMnTaGe compound. The muffin-tin sphere radii used in the calculations are 2.42, 2.42, 2.42, 2.28, and 2.25 (a.u), for Co, Mn, Ta, Si, and Ge, respectively. The following initial atomic configurations were employed: (Co $3d^7$ $4s^2$), (Mn $4s^2$ $3d^5$), (Ta $6s^2 5d^3$), (Si $3s^2$

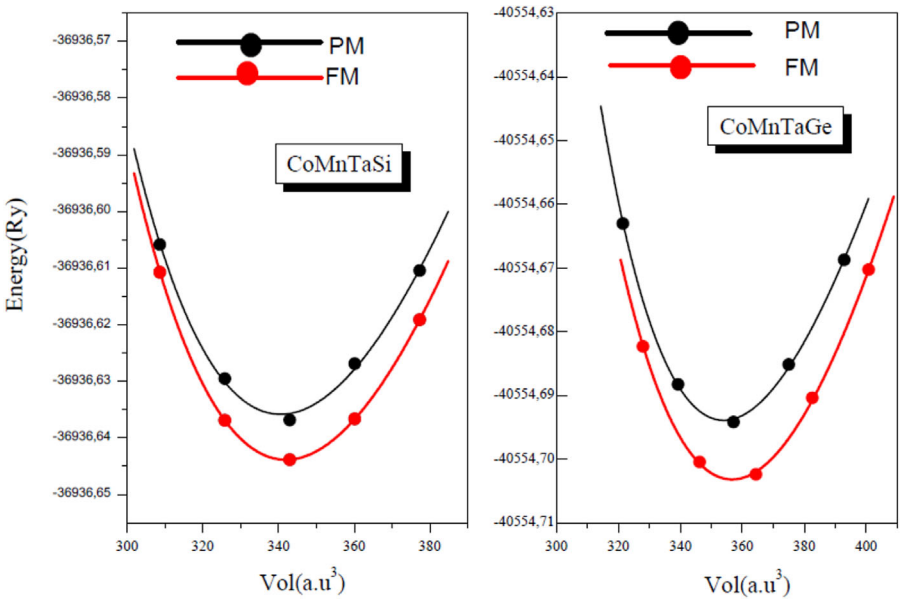

Figure 2 Volume optimization for the CoMnTaZ (Z = Si, Ge) Heusler compounds using GGA method.

Table 1 Lattice constant a (Å), bulk modulus B (in GPa), pressure derivative of bulk modulus B'.

compound	a	B	B'
CoMnTaGe(FM)	5.96	164.26	4.43
CoMnTaGe(PM)	5.95	194.90	3.48
CoMnTaSi(FM)	5.88	244.25	5.14
CoMnTaSi(PM)	5.87	237.46	5.60
CoMnCrSb(FM) [44]	6.067	140.5	5.25

Table 2 Formation energy of the CoMnTaSi and CoMnTaGe compounds.

compounds	E_f (Ry)
CoMnTaSi	−0.2418925
CoMnTaGe	−0.21370725

$3p^2$), and (Ge $4s^2$ $4p^2$). Self-consistent calculations are considered to be converged when the total energy of the system is stable within 10^{-6} Ry. The convergence criteria for total energy and force are taken as 10^{-5} and 10^{-6} eV Å^{-1}, respectively. The valence wave functions inside the spheres are expanded up to $l_{max} = 10$ while the charge density was Fourier expanded up to $G_{max} = 12$. The Monkhorst–Pack special k-points were performed using 3000 special k-points in the Brillouin zone [64].

3 Results and discussion In this subsection, we present the calculations of the total energy as a function of the unit-cell volume around the equilibrium compound in both paramagnetic and ferromagnetic states. As presented in the Fig. 2, structural optimization curves obtained in both FM and PM states. The calculated total energies are fitted to

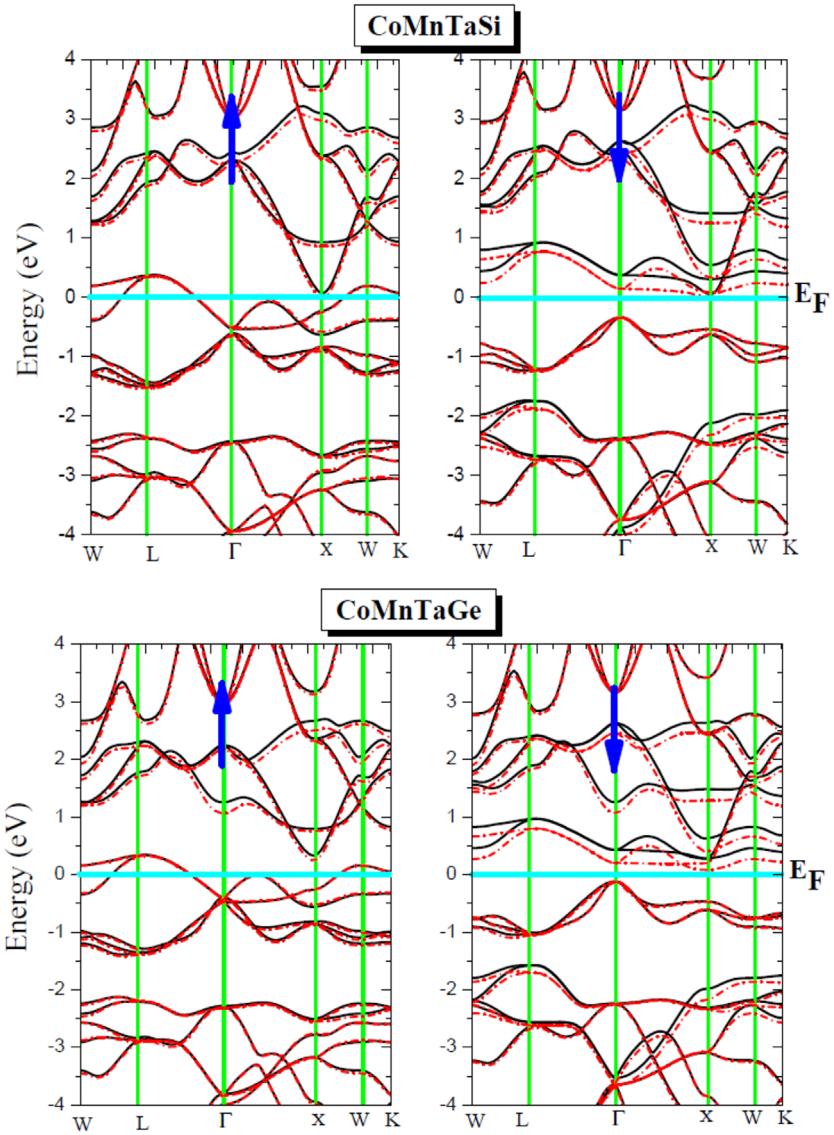

Figure 3 The band structure of the CoMnTaZ compounds for the spin-up and spin-down electrons, GGA+U(black line) and GGA (red line).

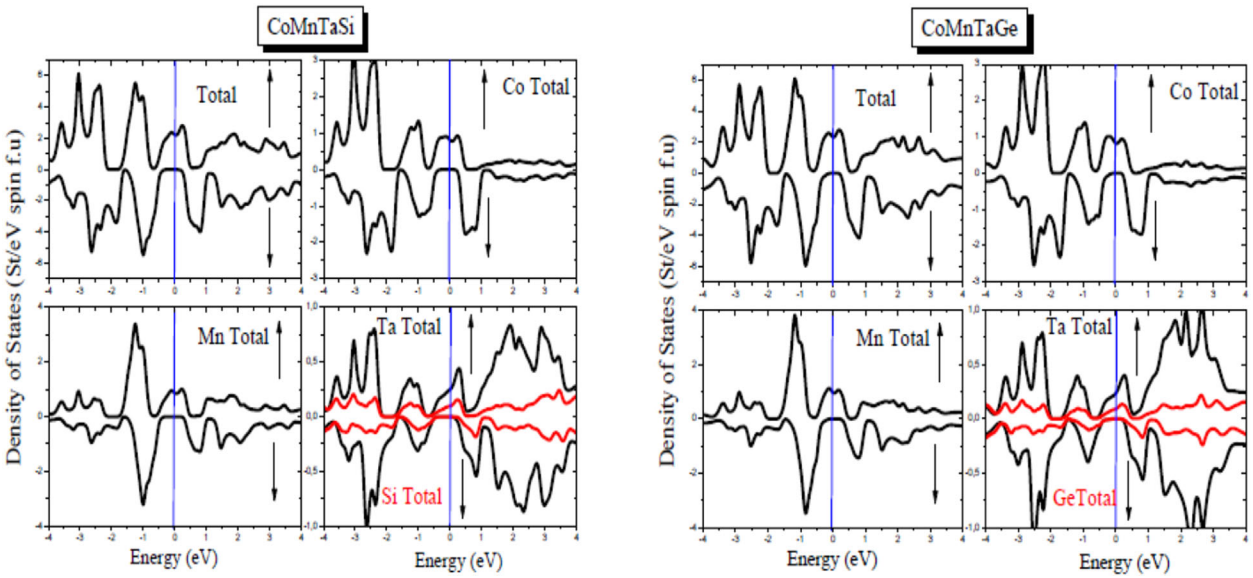

Figure 4 Spin-polarized total densities of states (TDOS) CoMnTaZ compounds using GGA+U method.

Murnaghan's equation of state (EOS) E–V [43], so as to determine the ground state properties, such as equilibrium lattice constant a (Å), bulk modulus B and its pressure derivative B'. The calculated structural parameters of CoMnTaZ (Z = Si, Ge) are reported in Table 1. To our knowledge there are no experimental data or theoretical calculations on the lattice constant, bulk modulus and its pressure derivative of these alloys. For comparison purpose, we also include in Table 1 the lattice constant, bulk modulus data for CoMnCrSb [44]. It is noticed that the bulk moduli

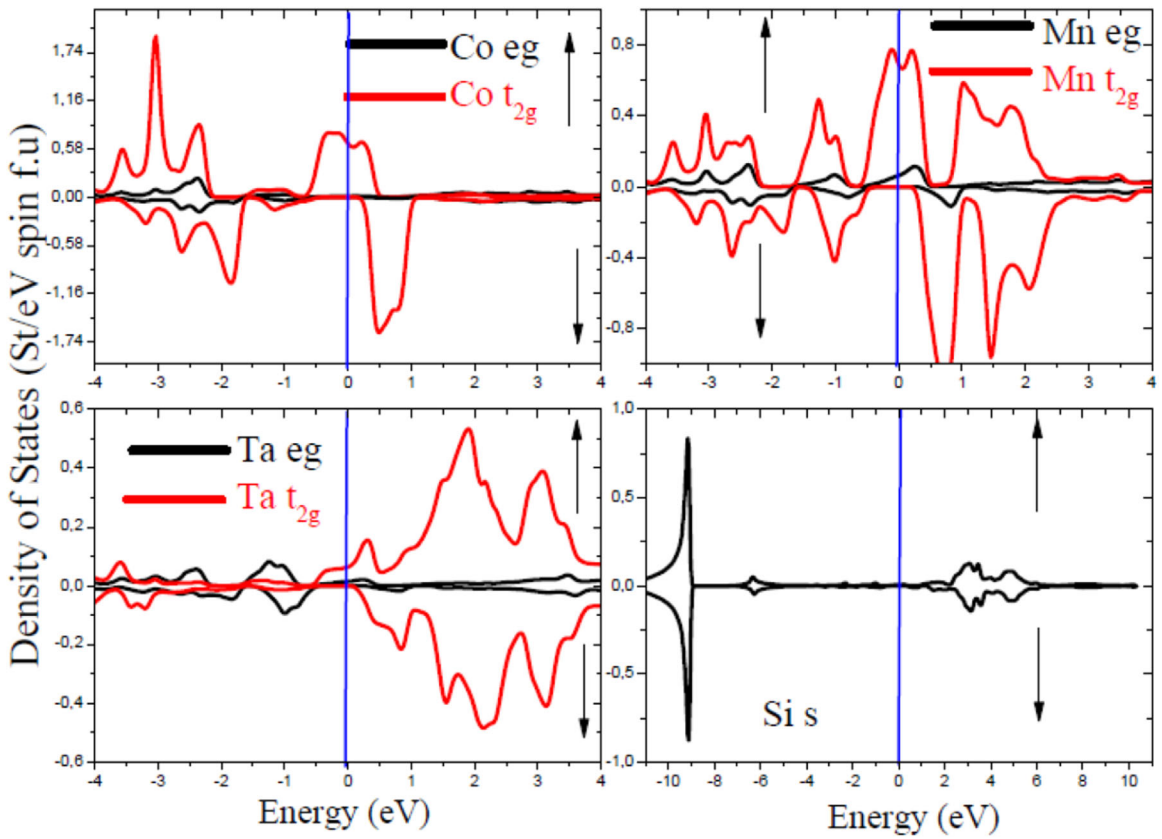

Figure 5 Spin-polarized partial densities of states (DOS) of CoMnTaZ compounds using GGA+U method.

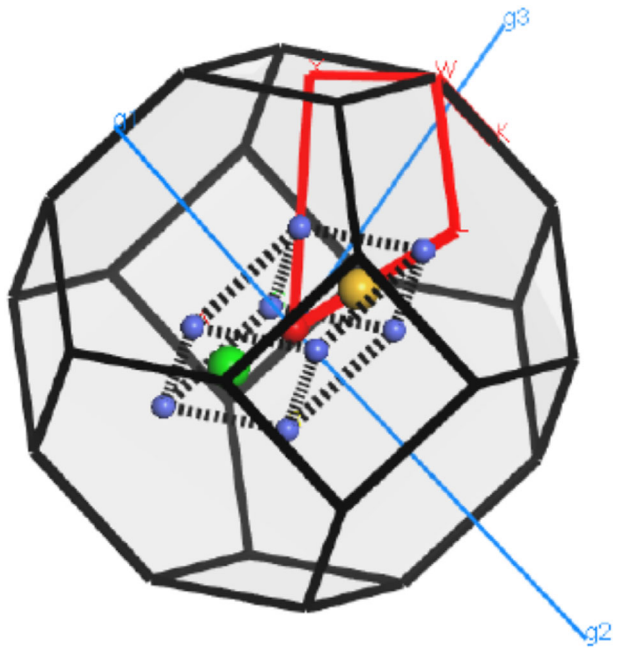

Figure 6 This is brillouin zone (BZ) indicating the high symmetry points for tetragonal structure, the path in direction of $W \rightarrow L \rightarrow \Gamma \rightarrow X \rightarrow W \rightarrow K$.

for the heusler are comparable with slight decreases from CoMnCrSb [44] to CoMnTaSi to CoMnTaGe, it is known that there is a strong correlation between the bulk modulus and hardness of materials; therefore, the herein considered materials possess practically the same degree of hardness. The bulk modulus of CoMnTaSi is larger than that of CoMnTaGe. This means that CoMnTaSi is a harder material than CoMnTaGe. At equilibrium lattice constant of 5.88 Å for CoMnTaSi and 5.96 Å for CoMnTaGe, the total energy of the magnetic phase is 0.106 and 0.125 eV f.u^{-1} for CoMnTaSi and CoMnTaGe, lower than that of the paramagnetic one.

The following equation defines the formation energy (E_f) for the CoMnTaSi and CoMnTaGa and determine the thermal stability of a compounds

$$E_f = E^{tot}_{CoMnTa(Si,Ge)} - \left[E^{bulk}_{Co} + E^{bulk}_{Mn} + E^{bulk}_{Ta} + E^{bulk}_{(Si,Ge)}\right] \quad (1)$$

where $E^{tot}_{CoMnTaSi}$ and $E^{tot}_{CoMnTaGe}$ are the equilibrium total energy calculated by first principles of the CoMnTaSi and CoMnTaGa compounds per formula unit and E^{tot}_{Co}, E^{tot}_{Mn}, E^{tot}_{Ta}, E^{tot}_{Si}, and E^{tot}_{Ge} correspond to the total energy per atom for the Co, Mn, Ta, Si, and Ge atoms, respectively. In Table 2, we have given the values of formation energy per formula unit of the CoMnTaSi and CoMnTaGe compounds. The negative values of formation energy indicate that the CoMnTaSi and CoMnTaGe compounds are energetically stable. The calculated values of the formation energy of the CoMnTaSi compound is more negative than those calculated for CoMnTaGa compounds, indicating the CoMnTaSi has a more stable CoMnTaGe compounds.

The self-consistent scalar relativistic band structures as well as density of states for the CoMnTaZ (Z = Si, Ge) along the various symmetry lines within the GGA and GGA+U scheme are given in Figs. 3–5, there is an overall topological resemblance for GGA and GGA+U methods. The majority spin band is metallic, while the minority spin band shows a semiconducting gap around the Fermi level. In the minority spin state, both compounds have the indirect energy band gap $\Gamma \rightarrow X$. Note, that the k-points in the desired k-paths were given within the zone boundary along the direction of $W \rightarrow L \rightarrow \Gamma \rightarrow X \rightarrow W \rightarrow K$ as shown in Fig. 6. These paths were derived from the base-centered tetragonal lattice BZ system.

The energy gap in the minority-spin band gap leads to 100% spin polarization at the Fermi level, resulting in the half-metallic behavior at equilibrium state. The energy band gap (Eg $\downarrow$ = 0.34 and 0.39 eV) in spin down channel for CoMnTaSi and CoMnTaGe compounds, respectively. The electron spin polarization (P) at the Fermi energy (E_F) of a material is defined by the following equation:

$$P = \frac{\rho\uparrow(E_F) - \rho\downarrow(E_F)}{\rho\uparrow(E_F) + \rho\downarrow(E_F)} \quad (2)$$

where $\rho\uparrow$ and $\rho\downarrow$ are the spin up and spin down density of states at the Fermi level E_F [65]. The similar results are also obtained by GGA+U calculation. We glad to see that half metallic properties remaining robust after the electron correlation is considered.

Figures 4 and 5 illustrate the total and partial density of states of CoMnTaSi compound at optimized geometry. In the Fig. 5, the density of states (DOS) of Co-e_g and t_{2g}, Mn-e_g and t_{2g}, Ta-e_g and t_{2g}, and Si-s electrons for the spin-up

Table 3 Total and partial magnetic moment (in μ_B) for CoMnTaSi and CoMnTaGe Heusler compounds.

compound	method	m_{Co}	m_{Mn}	$m_{Ta/Cr}$	interstitial	$m_{Ge/Si/Sb}$	m_{total}
CoMnTaGe	GGA	0.703	0.364	−0.016	−0.028	0.004	1.00
	GGA+U	0.704	0.362	−0.016	−0.032	0.002	1.00
CoMnTaSi	GGA	0.615	0.532	−0.060	−0.048	−0.002	1.00
	GGA+U	0.620	0.521	−0.060	−0.050	−0.003	1.00
CoMnCrSb [44]	GGA	1.14	3.17	−1.29	−0.069	0.02	3.00

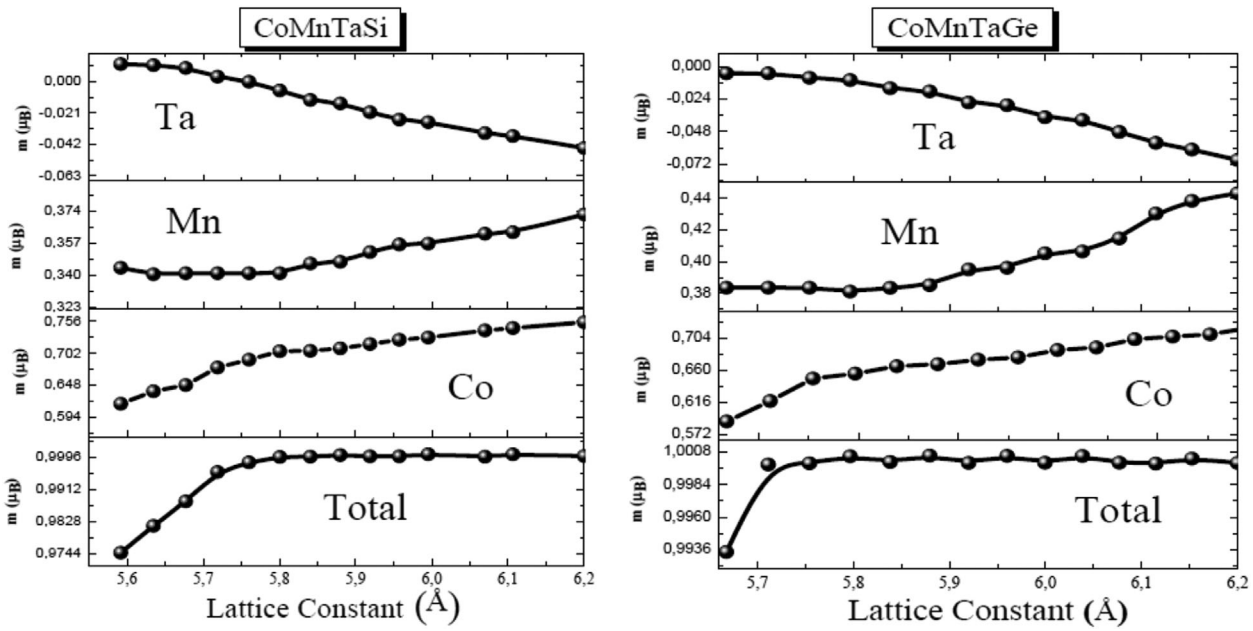

Fig. 7 The calculated total magnetic moment, the magnetic moments of the Co, Mn, and Ta atoms as a function of lattice constant.

and -down sub-bands, in both spin channels, significant contribution to the total density of states in the core states, come from s electrons of Si elements. At the Fermi energy, the situation is markedly different. Such a band structure is the signature of a half-metallic material, the hybridization bonding states Co-e_g and t_{2g}, Mn-e_g and t_{2g} element, one can see that the Co-t_{2g} and Mn-t_{2g} (spin-up) states are partially occupied, compared to the Mn-eg (spin-up) states are completely occupied. For unoccupied states above the Fermi level, the contribution of the Ta eg and t2g electrons is

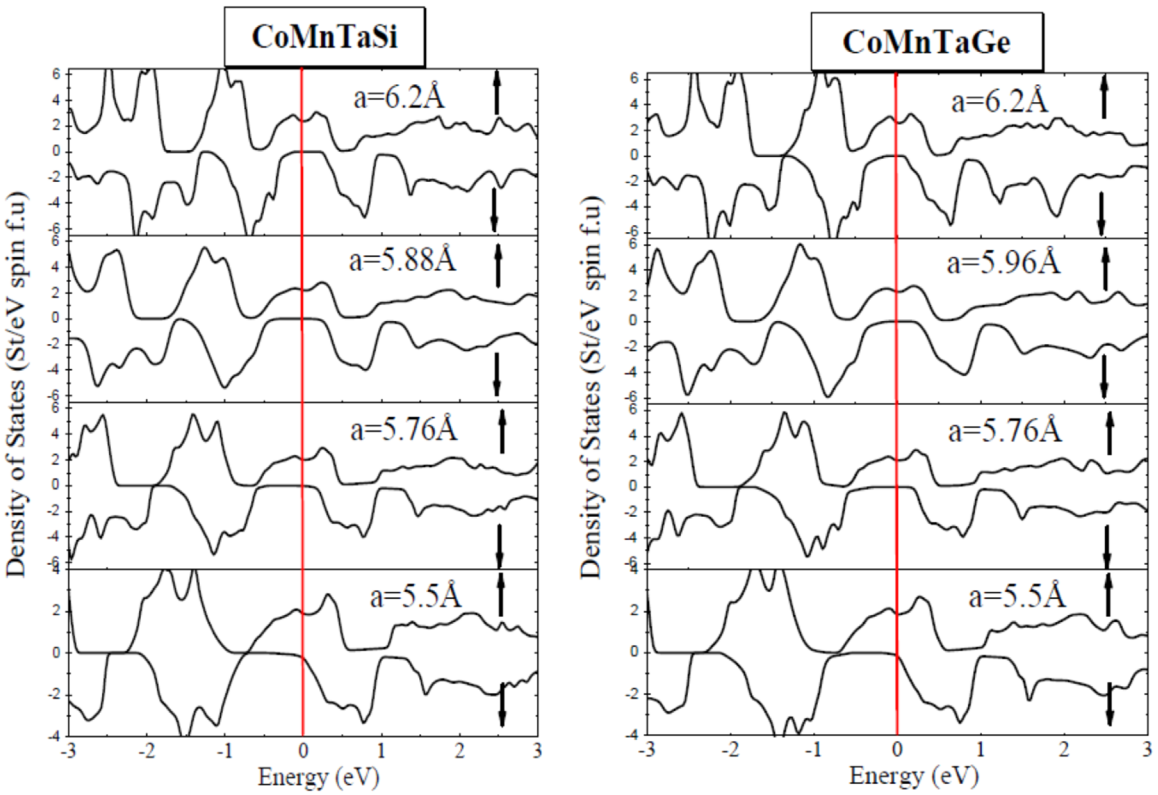

Fig. 8 Total TDOS for the CoMnTaZ quaternary Heusler compounds as a function of the lattice constant.

principally for the highest bands CB. These values of polarization are similar to those already published for TiZrCoSn quaternary Heusler compound calculated with a projector augmented-wave (PAW) pseudopotential [66].

The calculated total and atom-resolved magnetic moments of CoMnTaZ alloys are summarized in Table 3. The total spin moment is 1.00 μ_B for both the compounds in the GGA and GGA+U methods, which have 25 valence electrons per unit cell. Thus these compounds follow the Slater–Pauling behavior and the "rule of 24". The main contribution to the total magnetic moment is due to transition elements and the magnetic moment of silicon and germanium atoms is small. For Ta atoms for both methods, $-0.060\,\mu_B$ for CoMnTaSi atom and $-0.016\,\mu_B$ for CoFeMnGe atom. So the local moments changing, but the total moment being constant.

Özdoğan et al. [67] studied the electronic structure of the half-metals CoFeTiSi, CoCrVAs, and CoMnTiAs alloys using first-principle calculations, and found that the magnetic moment per cobalt atoms range from 0.58 to 0.72 μ_B. However, for CoMnTaSi and CoMnTaGe compounds, the magnetic moment of the manganese atoms are different from each other, indicating different atomic environments, for example, in the spin gapless semiconductors CoMnCrSi, the magnetic moment of the manganese atoms is $-0.77\,\mu_B$ [67], while in the half metallic CoMnCrSb is 3.17 μ_B [44], and 3.02 μ_B for CoFeMnGe [68].

In Fig. 7, we present detailed information on the atomic and total magnetic moments as a function of lattice constant. The calculated total magnetic moment is 1.00 μ_B for both compounds, in the range of 5.76–6.2 Å. For thus compounds, as can be seen, in the range of 5.5–5.76 Å, the m_{tot} is below the integer value of 1.00 μ_B. The calculated magnetic moments of the Co atoms increase with increase in lattice constant, while the magnetic moment of the Ta atoms decreases, and the magnetic moment of Mn atoms slightly increase with lattice constant.

In Fig. 8, the TDOS of CoMnTa (Si, Ge) at different lattice constants are presented. It is clearly seen in Fig. 8 that the CoMnTa (Si, Ge) Heusler compounds have half-metallic nature above the lattice constant value of 5.76 Å. Note that, for thus compounds, the energy band gap decreases with increase in lattice constant.

4 Conclusions For the CoMnTaZ (Z = Si, Ge) quaternary Heusler compounds, the electronic structure and magnetic properties compound have been calculated using the full-potential linearized augmented plane waves (FPLAPW) method as implemented in WIEN2k code. At the equilibrium lattice constant, the spin-polarized results show that CoMnTaZ (Z = Si, Ge) compounds has half-metallic ferromagnetic character with a total spin moment of 1.00 μ_B and the local moments changing, but the total moment being constant. The GGA calculation shows the CoMnTaSi and CoMnTaGe compounds at its equilibrium lattice constant are HM ferromagnet with an indirect band gap $\Gamma \rightarrow X$ of 0.34 and 0.39 eV and a HM gap of 0.34 and 0.13 eV in the spin-down channel. The CoMnTaZ (Z = Si, Ge) compounds have an integer total magnetic moment of 1.00 μ_B, satisfying the Slater–Pauling rule $m_{tot} = (Nv - 24)$. The half-metalliciy characteristic exists in relatively wide ranges of 5.76–6.2 Å. The similar results are also obtained by GGA+U calculation. These new materials are good candidates for potential applications in spintronic.

References

[1] S. A. Wolf, D. D. Awschalom, R. A. Buhrman, J. M. Daughton, S. von Molnar, M. L. Roukes, A. Y. Chtchelkanova, and D. M. Treger, Science **294**, 1488 (2001).
[2] G. A. Prinz, Science **282**, 1660 (1998).
[3] Y. Ohno, D. K. Young, B. Beshoten, F. Matsukura, H. Ohno, and D. D. Awschalom, Nature **402**, 790 (1999).
[4] T. Dietl, H. Ohno, F. Matsukura, J. Cibert, and D. Ferrand, Science **287**, 1019 (2000).
[5] J. H. Park, E. Voscovo, H. J. Kim, C. Kwon, R. Ramesh, and T. Venkatesh, Nature **392**, 794 (1998).
[6] Y. Sakuraba, M. Ueda, Y. Miura, K. Sato, S. Bosu, K. Saito, M. Shirai, T. J. Konno, and K. Takanashi, Appl. Phys. Lett. **101**, 252408 (2012).
[7] Y. Du, B. S. D. Ch., S. Varaprasad, Y. K. Takahashi, T. Furubayashi, and K. Hono, Appl. Phys. Lett. **103**, 202401 (2013).
[8] S. Li, Y. K. Takahashi, T. Furubayashi, and K. Hono, Appl. Phys. Lett. **103**, 042405 (2013).
[9] Y. K. Takahashi, S. Kasai, S. Hirayama, S. Mitani, and K. Hono, Appl. Phys. Lett. **100**, 052405 (2012).
[10] S. Shirotori, S. Hashimoto, M. Takagishi, Y. Kamiguchi, and H. Iwasaki, Appl. Phys. Express **8**, 023103 (2015).
[11] R. Farshchi and M. Ramsteiner, J. Appl. Phys. **113**, 191101 (2013).
[12] T. Kubota, S. Tsunegi, M. Oogane, S. Mizukami, T. Miyazaki, H. Naganuma, and Y. Ando, Appl. Phys. Lett. **94**, 122504 (2009).
[13] H. Liu, Y. Honda, T. Taira, K. Matsuda, M. Arita, T. Uemura, and M. Yamamoto, Appl. Phys. Lett. **101**, 132418 (2012).
[14] I. Zutic, J. Fabian, and S. D. Sarma, Rev. Mod. Phys. **76**, 323 (2004).
[15] A. Aguayo and G. Murrieta, J. Magn. Magn. Mater. **323**, 3013–3017 (2011).
[16] R. A. de Groot, F. M. Mueller, P. G. van Engen, and K. H. J. Bus-chow, Phys. Rev. Lett. **50**, 2024 (1983).
[17] T. S. Chan, R. S. Liu, G. Y. Guo, S. F. Hu, J. G. Lin, J. M. Chen, and C. R. Chang, Solid State Commun. **133**, 265 (2005).
[18] H. Wu, Phys. Rev. B **64**, 125126 (2001).
[19] H. T. Jeng and G. Y. Guo, Phys. Rev. B **67**, 1 (2003).
[20] H. Kato, T. Okuda, Y. Okimoto, Y. Tomioka, Y. Oikawa, K. Kamiyama, and T. Tokura, Phys. Rev. B **69**, 184412 (2004).
[21] I. V. Solovyev, J. Magn. Magn. Mater. **268**, 194 (2004).
[22] W. Song, J. Wang, and Z. Wu, Chem. Phys. Lett. **482**, 246 (2009).
[23] J. Wang, J. Wang, and Z. Wu, Chem. Phys. Lett. **501**, 324 (2011).
[24] S. E. A. Yousif and O. A. Yassin, J. Alloys Compd. **506**, 456 (2010).
[25] V. V. Bannikov, I. R. Shein, V. L. Kozhevnikov, and A. L. J. Ivanovsky, Struct. Chem. **49**, 781 (2008).

[26] S. Berri, J. Magn. Magn. Mater. **385**, 124–128 (2015).
[27] K. Kusakabe, M. Geshi, H. Tsukamoto, and N. Suzuki, J. Phys.: Condens. Matter **16**, 5639 (2004).
[28] O. Volnianska, P. Jakubas, and P Boguslawski, J. Alloys Compd. **423**, 191 (2006).
[29] M. Sieberer, J. Redinger, S. Khmelevskyi, and P. Mohn, Phys. Rev. B **73**, 024404 (2006).
[30] G. Y. Gao, K. L. Yao, E. Şaşıoğlu, L. M. Sandratskii, Z. L. Liu, and J. L. Jiang, Phys. Rev. B **75**, 174442 (2007).
[31] R. A. de Groot and K. H. J. Buschow, J. Magn. Magn. Mater. **1377**, 54–57 (1986).
[32] E. Kulatov and I. I. Mazin, J. Phys.: Condens Matter **2**, 343 (1990).
[33] J. S. Moodera and D. M. Mootoo, J. Appl. Phys. **76**, 6101 (1994).
[34] K. Schwarz, J. Phys. **F16**, L211 (1986).
[35] S. Matar, G. Demazeau, J. Sticht, V. Eyert, and J. Kűbler, J. Phys. I **2**, 315 (1992).
[36] H. van Leuken and R. A. de Groot, Phys. Rev. B **51**, 7176 (1995).
[37] S. P. Lewis, P. B. Allen, and T. Sasaki, Phys. Rev. B **55**, 10253 (1997).
[38] W. E. Pickett and D. J. Singh, Phys. Rev. B **53**, 1146 (1996).
[39] J. H. Park, E. Vescovo, H. J. Kim, C. Kwon, R. Ramesh, and T. Ventakesan, Nature (London) **392**, 6678 (1998).
[40] S. Berri, M. Ibrir, D. Maouche, and M. Attallah, Comput. Condensed. Mater. **1**, 26–31 (2014).
[41] S. Berri, M. Ibrir, D. Maouche, and M. Attallah, J. Magn. Magn. Mater. **371**, 106–111 (2014).
[42] S. Berri, D. Maouche, M. Ibrir, and F. Zerarga, J. Magn. Magn. Mater. **354**, 65–69 (2014).
[43] M. H. Elahmar, H. Rached, D. Rached, R. Khenata, G. Murtaza, S. Bin Omran, and W. K. Ahmed, J. Magn. Magn. Mater. **393**, 165–174 (2015).
[44] S. Berri, J. Supercond. Nov. Magn. **29**, 1309. (2016). https://doi.org/10.1007/s10948-016-3404-7.
[45] M. Khodami and F. Ahmadian, J. Supercond. Nov. Magn. **28**, 3027–3035 (2015).
[46] Y. C. Gao, Y. Zhang, and X. T. Wang, J. Korean Phys. Soc. **66**, 959. (2015). https://doi.org/10.3938/jkps.66.959.
[47] M. N. Rasool, S. Mehmood, M. A. Sattar, M. A. Khan, and A. Hussain, J. Magn. Magn. Mater. **395**, 97–108. (2015).
[48] Y. J. Zhang, Z. H. Liu, G. T. Li, X. Q. Ma, and G. D. Liu, J. Alloys Compd. **616**, 449–453 (2014).
[49] P. Yan, J. Zhang, and K. Xu, Solid State Commun. **231–232**, 64–67 (2016).
[50] K. Benkaddour, A. Chahed, A. Amar, H. Rozale, A. Lakdja, O. Benhelal, and A. Sayede, J. Alloys Compd. **687**, 211–220 (2016).
[51] X. Wang, Z. Cheng, J. Wang, L. Wang, Z. Yu, Ch. Fang, J. Yang, and G. Liu, RSC Adv. **6**, 57041–57047 (2016).
[52] P.-L. Yan, J.-M. Zhang, B. Zhou, and K.-W. Xu, J. Phy. D Appl. Phys. **49**, 255002 (2016).
[53] H.-H. Xie, Q. Gao, L. Li, G. Lei, G.-Y. Mao, X.-R. Hu, and J.-B. Deng, Comput. Mater. Sci. **103**, 52–55 (2015).
[54] X. Wang, Z. Cheng, J. Wang, X. Wang, and G. Liu, J. Mater. Chem. C **4**, 7176 (2016).
[55] X. Wang, Z. Cheng, J. Wang, and G. Liu, J. Mater. Chem. C **4**, 8535 (2016).
[56] L. Y. Wang, X. T. Wang, R. K. Guo, T. T. Lin, and G. D. Liu, Solid State Commun. **244**, 38–42 (2016).
[57] X. Wang, Z. Cheng, R. Guo, J. Wang, H. Rozale, L. Wang, Z. Yu, and G.g Liu, Mater. Chem. Phys. **193**, 99–108 (2017).
[58] R. Guo, G. Liu, X. Wang, H. Rozale, L. Wang, R. Khenata, Z. Wu, and X. Dai, RSC Adv. **6**, 109394–109400 (2016).
[59] G. K. H. Madsen, P. Blaha, K. Schwarz, E. Sjöstedt, and L. Nordström, Phys. Rev. B **64**, 195134 (2001).
[60] K. Schwarz, P. Blaha, and G. K. H. Madsen, Comput. Phys. Commun. **147**, 71 (2002).
[61] P. Blaha, K. Schwarz, G. K. H. Madsen, D. Kvasnicka, and J. Luitz, WIEN2K, an Augmented Plane Wave +Local Orbitals Program for Calculating Crystal Properties (Karlheinz Schwarz, Technische Universität, Wien, Austria, 2001) ISBN 3-9501031-1-2.
[62] J. P. Perdew, S. Burke, and M. Ernzerhof., Phys. Rev. Lett. **77**, 3865 (1996).
[63] V. I. Anisimov, J. Zaanen, and O. K. Andersen, Phys. Rev. **B44**, 943 (1991).
[64] H. J. Monkhorst and J. D. Pack, Phys. Rev. B **13**, 5188 (1976).
[65] R. J. Soulen, Jr., J. M. Byers, M. S. Osofsky, B. Nadgorny, T. Ambrose, S. F. Cheng, P. R. Broussard, C. T. Tanaka, J. Nowak, J. S. Moodera, A. Barry, and J. M. D. Coey, Science **282**, 85 (1998).
[66] X.-H. Kang and J.-M. Zhang, J. Phys. Chem. Solids **105**, 9–15 (2017).
[67] K. Özdoğan, E. Şaşıoğlu, and I. Galanakis, J. Appl. Phys. **113**, 193903 (2013).
[68] K. Seema, AIP Conf. Proc. **1731**, 130049 (2016). https://doi.org/10.1063/1.4948155.

